

Quantum state preparation without coherent arithmetic

Sam McArdle,^{1,2} András Gilyén,³ and Mario Berta^{1,2,4}

¹*AWS Center for Quantum Computing, Pasadena, CA 91125, USA*

²*Institute for Quantum Information and Matter,
California Institute of Technology, Pasadena, USA**

³*Alfréd Rényi Institute of Mathematics, Budapest, Hungary[†]*

⁴*Department of Computing, Imperial College London, London, UK[‡]*

(Dated: October 27, 2022)

We introduce a versatile method for preparing a quantum state whose amplitudes are given by some known function. Unlike existing approaches, our method does not require handcrafted reversible arithmetic circuits, or quantum memory loads, to encode the function values. Instead, we use a template quantum eigenvalue transformation circuit to convert a low cost block encoding of the sine function into the desired function. Our method uses only 4 ancilla qubits (3 if the approximating polynomial has definite parity), providing order-of-magnitude qubit count reductions compared to state-of-the-art approaches, while using a similar number of Toffoli gates if the function can be well represented by a polynomial or Fourier approximation. Like black-box methods, the complexity of our approach depends on the ‘L2-norm filling-fraction’ of the function. We demonstrate the efficiency of our method for preparing states commonly used in quantum algorithms, such as Gaussian and Kaiser window states.

I. INTRODUCTION

Problem setting. We seek to prepare an $N = 2^n$ dimensional quantum state on n qubits with amplitudes described by a function $f: [a, b] \rightarrow \mathbb{C}$ defined as

$$|\Psi_f\rangle := \frac{1}{\mathcal{N}_f} \sum_{x=0}^{N-1} f(\bar{x})|x\rangle, \quad (1)$$

where $\bar{x} := ((b-a)x/N + a)$,¹ and $\mathcal{N}_f := \sqrt{\sum |f(\cdot)|^2}$. Such states are used in many quantum algorithms, including: basis and boundary functions in finite element analysis [1, 2] or differential equations [3–5], states in quantum simulations of field theories [6, 7], payoff and price distribution functions for financial derivative pricing [8, 9], priors for phase estimation [10], and radial and angular electron-orbital wave-functions in grid-based quantum chemistry simulations [11, 12]. Typical preparation methods [13–16] require an amplitude oracle $|x\rangle|0\rangle \rightarrow |x\rangle|f(\bar{x})\rangle$ that prepares a k -bit approximation of $f(\bar{x})$ (or some closely related oracle [17–19]). This can be implemented either by coherent arithmetic [20–22], or by reading values stored in a quantum memory (which may be cheaper for small system sizes [23]). Both have high qubit and gate costs. Coherent arithmetic circuits are typically constructed by hand, to minimize resources and incorporate the nuances of fixed-point arithmetic, such as overflow errors [22]. Our approach does not use an amplitude oracle, saving considerable resources. This

is vital in the early fault-tolerant regime, where we need to minimize the footprint of quantum algorithms [24–27].

Framework. Our method uses quantum eigenvalue transformation (QET) [28–31] — or more generally quantum singular value transformation (QSVT) [31] — a technique to coherently apply (non-unitary) functions to the eigenvalues of a block-encoded Hermitian matrix.² An $(n+m)$ -qubit unitary U is said to be an (α, m, ϵ) -block-encoding of an n -qubit Hermitian matrix A if

$$\left\| \alpha \langle 0|^{\otimes m} \otimes I_n U (|0\rangle^{\otimes m} \otimes I_n) - A \right\| \leq \epsilon. \quad (2)$$

The default QET/QSVT approach [31, 33] uses $d/2$ applications of U and of U^\dagger , $2d$ m -controlled Toffoli gates (which are just CNOT gates for the $m = 1$ case herein), d single-qubit Z -rotations of an additional ancilla qubit, and two Hadamard gates in order to block-encode a degree d real and definite-parity polynomial of A . Using linear combinations of block encodings [31], we can block-encode complex, mixed-parity functions. For the real mixed-parity case, we need one more ancilla qubit and one application of U needs to be controlled by it. Also, the rotation gates need to be controlled and we need $2d$ of them together with 4 Hadamard gates [31, 33] (and the normalization is decreased by one half).

Approach. As shown in Fig. 1, we use QET to convert a low-cost block encoding of $A := \sum_x \sin(x/N)|x\rangle\langle x|$,

* sam.mcardle.science@gmail.com

† gilyen@renyi.hu

‡ bertamario@gmail.com

¹ When a more symmetric discretization of $[a, b]$ is desired, one can, for example, replace the factor of $(b-a)$ by $(b-a)N/(N-1)$, but we ignore such details for clarity of exposition here.

² We use the following conventions [32]: quantum signal processing (QSP) describes polynomial transformations applied to a scalar value encoded in a single-qubit operator [28–30], quantum eigenvalue transformation (QET) lifts QSP to transform the eigenvalues of multiqubit Hermitian matrices [29–31], and quantum singular value transformation (QSVT) extends QET to non-Hermitian matrices [31], providing a unifying framework for QSP, QET, and many existing quantum algorithms.

into a block-encoding of $\sum_x f(\bar{x})|x\rangle\langle x|$,³ using a polynomial approximation of $f((b-a)\arcsin(\cdot) + a)$. Our approach is well suited to functions with a low-degree polynomial (or as we show later, Fourier series) approximation, and it provides order-of-magnitude reductions in the number of ancilla qubits required. Unlike amplitude-oracle-based approaches, we avoid discretizing the values the function can take, providing instead a continuous approximation to the function. Our method is straightforward and versatile, as the same circuit template can be used for a wide range of functions.

Outline. In Sec. II we describe our method for QET-based state preparation, with our main result presented in Theorem 1. In Sec. III we discuss the complexity of our method for preparing Gaussian and Kaiser window functions commonly used in quantum algorithms. We present concrete resource estimates for our approach, and compare to state-of-the-art methods in Sec. IV. Finally, in Sec. V we give extensions for dealing with discontinuities, using improved priors, and preparing functions with Fourier-based QET.

II. MAIN RESULT

Classical pre-computation. The function we seek to implement using QET is

$$h(y) := f((b-a)\arcsin(y) + a) \quad (3)$$

over the domain $y \in [0, \sin(1)]$. Because the QET/QSVT framework imposes $|h(y)| \leq 1$, we rescale the function

$$\hat{h}(y) := \frac{h(y)}{|h(y)|_{\max}^{y \in [0, \sin(1)]}}. \quad (4)$$

where $|\cdot|_{\max}^{[a,b]}$ denotes the maximum value the function can take on the interval $[a, b]$.

We use a degree d polynomial to approximate the (mixed-parity, real) function $\hat{h}(y)$. One can calculate the approximating minimax polynomials using the Remez algorithm [34, 35], or consider manual methods such as a Taylor expansion of $h(y)$. Approximating polynomials for common functions have been determined in previous works on QSVT [31, 32]. We refer to the actually implemented approximate function as $\tilde{f}(\bar{x})$. The degree d of the QET polynomial is chosen such that

$$\left| \frac{\tilde{f}(\bar{x})}{|\tilde{f}|_{\max}} - \frac{f(\bar{x})}{|f|_{\max}} \right|_{\max}^{\bar{x} \in [a,b]} \leq \delta. \quad (5)$$

In Appendix B we analyze how the error in the function approximation propagates to the final state. For this we

need to pre-compute additional quantities and we define a discretized and scaled 2-norm that approximates the continuous 2-norm of the function when N is large

$$\begin{aligned} \|\tilde{f}\|_2^{[N]} &:= \sqrt{\frac{(b-a)}{N} \sum_{x=0}^{N-1} |\tilde{f}(\bar{x})|^2} \\ &\approx \sqrt{\int_a^b |\tilde{f}(\bar{x})|^2 d\bar{x}} =: \|\tilde{f}\|_2^{[\infty]}, \end{aligned} \quad (6)$$

as well as a ‘discretized L2-norm filling-fraction’ that approximates the continuous L2-norm filling-fraction

$$\begin{aligned} \mathcal{F}_{\tilde{f}}^{[N]} &:= \frac{\|\tilde{f}\|_2^{[N]}}{\sqrt{(b-a)|\tilde{f}|_{\max}^2}} \\ &\approx \frac{\|\tilde{f}\|_2^{[\infty]}}{\sqrt{(b-a)|\tilde{f}|_{\max}^2}} =: \mathcal{F}_{\tilde{f}}^{[\infty]}. \end{aligned} \quad (7)$$

To bound the trace distance for the final state, we can either use $\mathcal{F}_{\tilde{f}}^{[N]}$ & $\mathcal{F}_{\tilde{f}}^{[N]}$ to compute rigorous asymptotic bounds (Appendix B), or we can use $\sum_x f(\bar{x})\tilde{f}(\bar{x})$ to compute a tighter bound in practice (Appendix B1). When N is small, these terms can be evaluated directly, while when N is large we approximate them by their continuous variants (e.g. $\mathcal{F}_{\tilde{f}}^{[\infty]}$). Finally, given the degree d polynomial approximation, we can use efficient algorithms [33, 36, 37] to find the QET rotation angles.

Quantum algorithm. The quantum circuit for our state preparation routine is shown in Fig. 1.

In Fig. 1a, we apply n controlled-Y rotations of an ancilla qubit, and an X gate on the ancilla qubit, which performs

$$U_{\sin}|x\rangle_n|0\rangle_a \rightarrow |x\rangle_n(\sin(x/N)|0\rangle_a + \cos(x/N)|1\rangle_a). \quad (8)$$

The circuit U_{\sin} is a $(1, 1, 0)$ -block-encoding of $A = \sum_x \sin(x/N)|x\rangle\langle x|$.

The classically pre-computed QET circuit $U_{\tilde{f}}$ is shown in Fig. 1b, and acts on two additional ancilla qubits (one if \tilde{f} is of definite parity). The circuit $U_{\tilde{f}}$ applies the approximation of $\hat{h}(y)$ to the block-encoding of A , thus implementing a $(1, 3, 0)$ block-encoding of

$$\sum_{x=0}^{N-1} \frac{\tilde{f}(\bar{x})}{2|\tilde{f}(\bar{x})|_{\max}^{\bar{x} \in [a,b]}} |x\rangle\langle x|. \quad (9)$$

The circuit makes $d/2$ calls to U_{\sin} and to U_{\sin}^\dagger , and uses $2d$ controlled R_z gates, and $2d$ CNOT gates.

Applying $U_{\tilde{f}}$ to the initial state $|+\rangle^{\otimes n}|000\rangle_a$, the success probability of outputting $|\Psi_{\tilde{f}}\rangle|000\rangle_a$ is given by $\frac{\mathcal{N}_{\tilde{f}}^2}{4N|\tilde{f}|_{\max}^2} = \left(0.5\mathcal{F}_{\tilde{f}}^{[N]}\right)^2$. We then use $\mathcal{O}\left(1/\mathcal{F}_{\tilde{f}}^{[N]}\right)$ rounds of exact amplitude amplification (see Theorem 4) to boost the success probability to 1. Exact amplitude amplification introduces an additional qubit to adjust the

³ For an even / odd $f: [-a, a] \rightarrow \mathbb{C}$ we use the block-encoding $A := \sum_{x=-\frac{N}{2}}^{\frac{N}{2}-1} \sin(2x/N)|x\rangle\langle x|$ and approximate $f(a \arcsin(\cdot))$.

	# Non-Clifford gates	# Ancilla qubits	Avoids amplitude oracle	Rigorous error bounds	Comments
QET-based (This work)	$\mathcal{O}\left(\frac{n \cdot d_\epsilon}{\mathcal{F}_f^{[N]}}\right)$	4	✓	✓	Requires polynomial or Fourier series approximation
Black-box [13–15, 18, 19]	$\mathcal{O}\left(\frac{g_\epsilon^2 \cdot \tilde{d}_\epsilon}{\mathcal{F}_f^{[N]}}\right)$	$\mathcal{O}(g_\epsilon \tilde{d}_\epsilon)$	✗	✓	Generally applicable
Grover-Rudolph [17]	$\mathcal{O}(ng_\epsilon^2 \tilde{d}_\epsilon)$	$\mathcal{O}(g_\epsilon \tilde{d}_\epsilon)$	✗	✓	Function must be efficiently integrable probability distribution
Adiabatic state preparation [16]	$\mathcal{O}\left(\frac{g_\epsilon^2 \cdot \tilde{d}_\epsilon}{(\mathcal{F}_f^{[N]})^4 \epsilon^2}\right)$	$\mathcal{O}(g_\epsilon \tilde{d}_\epsilon)$	✗	✓	Generally applicable
Matrix product state encoding [38, 39]	$\mathcal{O}(n)$	0	✓	✗	Function can be approximated by bond-dimension = 2 MPS

TABLE I. Comparing different methods to prepare quantum states representing continuous functions. We use the notation X_ϵ to indicate that a parameter depends on ϵ , the error in the state. We assume all approaches using an amplitude oracle instantiate it with the coherent arithmetic approach of [22]. This approach produces a g -bit discretization of $f(\bar{x})$ using a degree \tilde{d} piecewise polynomial approximation. Both g and \tilde{d} depend on the accuracy required in the function. The oracle uses $\mathcal{O}(g_\epsilon^2 \tilde{d}_\epsilon)$ Toffoli gates, and $\mathcal{O}(g_\epsilon \tilde{d}_\epsilon)$ logical qubits.

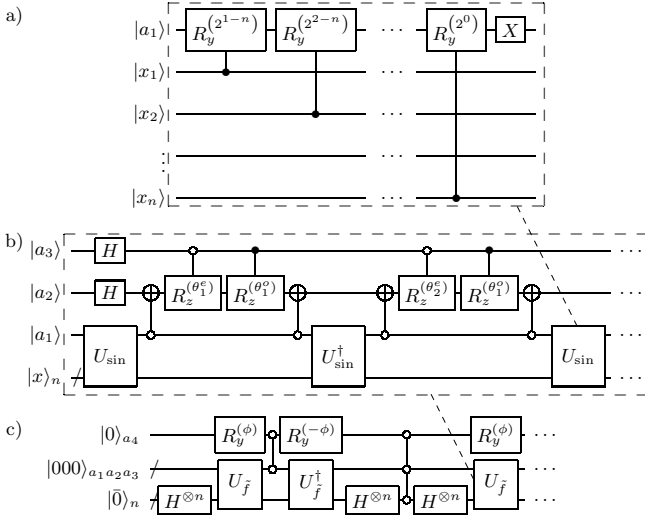


FIG. 1. The quantum circuit implementing QET-based state preparation. a) The circuit U_{\sin} that block-encodes $\sum_x \sin(x/N)|x\rangle\langle x|$. b) The circuit $U_{\tilde{f}}$ that block-encodes a sub-normalized version of $\sum_x \tilde{f}(\bar{x})|x\rangle\langle x|$. The angles $\theta_i^{e/o}$ correspond to the pre-computed QET-angles for the desired even/odd polynomials. c) The (exact) amplitude-amplification circuit which block encodes $\sum_x \tilde{f}(\bar{x})|x\rangle\langle 0|$, including an additional qubit to adjust the amplitude for amplification, as described in Appendix A.

amplitude by a factor of $\cos(\phi/2)$ such that it can be amplified with an integer number of rounds. We discuss in Appendix A 1 how to proceed if we can only approximate $\mathcal{F}_f^{[N]}$. The circuit for amplitude amplification is shown in Fig. 1c. Each round requires: one call to each of $U_{\tilde{f}}, U_{\tilde{f}}^\dagger$, a 4 qubit (anti)-controlled-Z gate (reflection around the desired state), an $(n+4)$ qubit (anti)-controlled-Z gate (reflection around the initial state), n Hadamard gates, and two $R_y^{(\pm\phi)}$ gates.

Complexity analysis. Using the rigorous error analysis in Appendix B and the above discussion gives the following theorem:

Theorem 1. *Given a polynomial of degree d_δ that (when applied to $\sin(x/N)$) approximates $f(\bar{x})/|f|_{\max}$ to L_∞ -error $\delta = \epsilon \cdot \text{Min}(\mathcal{F}_f^{[N]}, \mathcal{F}_{\tilde{f}}^{[N]})$, we can prepare a quantum state $|\Psi_{\tilde{f}}\rangle$ that is ϵ -close in trace-distance to $|\Psi_f\rangle$ using*

$$\mathcal{O}\left(\frac{n \cdot d_\delta}{\mathcal{F}_f^{[N]}}\right) \text{ gates.} \quad (10)$$

We require 4 ancilla qubits (3 if \tilde{f} has definite parity); 1 to block-encode $\sin(x)$, 2 for QET (1 if definite parity), and 1 for amplitude amplification. The constant factor hidden by the big- \mathcal{O} notation is function dependent, and may depend on the scaling factor $(b-a)$. For smooth functions that can be well approximated by polynomials, one can typically get an L_∞ -error δ decaying as $\mathcal{O}(\exp(-d))$ for a degree d approximating polynomial. We prove this formally in Appendix D resulting in the following:

Theorem 2. *Let $b > 0$ and $f(x_0 + x) = \sum_{k=0}^\infty a_k x^k$ for every $x \in (-b, b)$ and suppose $\sum_{k=0}^\infty |a_k| b^k \leq B$. Then $g(y) := f(x_0 + \frac{2b}{\pi} \arcsin(y)) = \sum_{k=0}^\infty c_k y^k$ is such that $\sum_{k=0}^\infty |c_k| \leq B$, thus for $\nu \in (0, 1]$ and $T \geq \ln(B/\delta)/\nu$ we have for all $y \in [-1 + \nu, 1 - \nu]$:*

$$\left| g(y) - \sum_{k=0}^{T-1} c_k y^k \right| \leq \delta.$$

Hence, we can then prepare a quantum state $|\Psi_{\tilde{f}}\rangle$ that is ϵ -close in trace-distance to $|\Psi_f\rangle$ using

$$\tilde{\mathcal{O}}\left(\frac{n}{\mathcal{F}_f^{[N]}} \log\left(\frac{1}{\epsilon}\right)\right) \text{ gates,} \quad (11)$$

where the notation $\tilde{\mathcal{O}}(\cdot)$ hides poly-logarithmic terms. We show how Theorem 2 applies to Gaussian and Kaiser window functions in Sec. III. As N is increased, $\mathcal{F}_{\tilde{f}}^{[N]} \rightarrow \mathcal{F}_{\tilde{f}}^{[\infty]}$, a constant value independent of N , for a given function. Furthermore, in practice the error analysis can be tightened, as discussed in Appendix B 1.

Comparison. We contrast the scaling and features of our method with existing approaches in Table I. Although we have used big- \mathcal{O} notation to simplify the presentation, the constant factors in our method are modest (as shown by our resource estimates in Sec. IV). Our method uses the fewest ancilla qubits of all methods with rigorous error bounds, and has improved non-Clifford gate complexity compared to the black-box and adiabatic state preparation approaches for typical values of $n, d_\epsilon, g_\epsilon, \tilde{d}_\epsilon$ [22] (parameters specified in the caption of Table I). While the Grover-Rudolph (GR) method has a gate complexity independent of the L2-norm filling-fraction, it is only applicable to functions representing efficiently integrable probability distributions (and as we will see in Sec. IV typically requires a large number of ancilla qubits for working registers). While the heuristic matrix product state approach appears promising for approximating simple functions on near-term quantum devices, it is currently unclear whether that approach can achieve high accuracy and favorable scaling for more complicated functions.

III. APPLICATIONS

We apply our algorithm to prepare functions with important applications in quantum algorithms: Kaiser window and Gaussian functions. The Kaiser window function $W_\beta(x) = \frac{I_0(\beta\sqrt{1-x^2})}{I_0(\beta)}$ (where I_0 is the zeroth modified Bessel function of the first kind, see Appendix C) can be used in quantum phase estimation [10] (the ancilla qubits are prepared in this state, rather than uniformly) to boost the success probability without having to (coherently) calculate the median of several phase evaluations (see discussion in [40]). Gaussian states $f_\beta(x) = \exp(-\frac{\beta}{2}x^2)$ are widely used in quantum algorithms, e.g. in chemistry [12, 41], simulation of quantum field theories [6, 7], and finance [8, 9]. In Appendix F we prove the following theorem on the complexity of preparing Gaussian⁴ and Kaiser window states:

Theorem 3. *Let $f_\beta(x)$ be either $\exp(-\frac{\beta}{2}x^2)$ or $W_\beta(x)$. If $\epsilon \in (0, \frac{1}{2})$ and $2^n \geq \sqrt{\beta} \geq 0$, then we can prepare the corresponding Gaussian / Kaiser window state on n qubits up to ϵ -precision with gate complexity*

$$\mathcal{O}\left(n^4\sqrt{\beta+1}(\beta+\log(1/\epsilon))\right). \quad (12)$$

For Gaussian states $f_\beta(x) = \exp(-\frac{\beta}{2}x^2)$ if $\beta \geq \log(1/\epsilon)$ this complexity can be further improved to

$$\mathcal{O}\left(n\log^{\frac{5}{4}}(1/\epsilon)\right). \quad (13)$$

Kaiser window state. The (unnormalised) Kaiser window state is given by

$$|W_\beta(\bar{x})\rangle = \sum_{x=-N}^N \frac{1}{2N} \frac{I_0(\beta\sqrt{1-\bar{x}^2})}{I_0(\beta)} |x\rangle \quad (14)$$

for $\bar{x} \in [-1, 1]$. The parameter β controls the trade-off between the central-band width and side-band height when viewed in the Fourier domain.

In Appendix D we show that $W_\beta(\arcsin(\bar{x}))$ can be approximated by a degree $\mathcal{O}(\beta + \ln(\delta^{-1}))$ polynomial on the interval $x \in [-\sin(1), \sin(1)]$, utilizing the fact that $W_\beta(x)$ has a nicely behaving Taylor series. To bound the filling-fraction, we show in Appendix E that $W_\beta(x) \geq 1 - \beta x^2/2$. By integrating the lower bound for $\beta \geq 2$ we get that $\int_{-1}^1 W_\beta(x)^2 dx \geq \sqrt{2/\beta}$. Hence $\mathcal{F}_{W_\beta}^{[\infty]} \geq \beta^{-1/4}$. This lower bound appears tight in practice, matching the true value with 85-90% accuracy. Putting these bounds together with Theorem 1 gives the stated complexity in Eq. (12).

For application in phase estimation, we can relate β to the probability of failure η as $\beta \sim \ln(\eta^{-1})$, and n to the precision ϵ_ϕ of phase estimation as $n \sim \log(\epsilon_\phi^{-1} \ln(\eta^{-1}))$ [10]. Hence, our method scales poly-logarithmically in all parameters. We are not aware of any prior work discussing the complexity of preparing the Kaiser window state (which is also omitted from [10]) or of resource estimates for implementing an amplitude oracle of the Bessel function, that could be used for the black-box or adiabatic state preparation methods.

Gaussian state. The proof of Theorem 3 for the Gaussian case is completely analogous to the Kaiser window case above. The bound can be tightened by observing that Gaussian functions take values close to zero for large x values, and so one can assume without loss of generality that $\beta = \mathcal{O}(\log(1/\epsilon))$, see Appendix F).

We contrast our method with bespoke approaches that only prepare Gaussians. The Kitaev-Webb (KW) method [42] can be viewed as a Gaussian-specific version of the GR method. It uses coherent arithmetic to evaluate a function involving arcsin, and square root, requiring a large number of ancilla qubits when instantiated using the piecewise polynomial oracle [22]. It was shown in [43] that the gate counts of the KW method were higher than those of exponentially scaling state preparation techniques [44] for modest $n \leq 16$. We also compare to the Gaussian-specific repeat-until-success approach of [45], which has a circuit depth of $\mathcal{O}(n^2)$ multiplied by the number of rounds of amplitude amplification used to boost the success probability to unity (bounded by a large constant value). The use of amplitude amplification requires at least n ancilla qubits here. The

⁴ Here β should be thought of as $\frac{1}{\sigma^2}$, the inverse of the variance.

error in the resulting function was not analysed explicitly, but appears to scale as $Poly(\epsilon^{-1})$ from numerical simulations [45].

We can also compare to the generic black-box, adiabatic state preparation, and GR methods. The first two require an oracle for the Gaussian function. Using the piecewise polynomial oracle with a target error of $L_\infty = 10^{-5}$ uses 133 ancilla qubits [22]. The GR approach would require an oracle for the *error function* (*erf*), which is likely even more costly.

IV. RESOURCE ESTIMATES

Example. For an in-depth quantitative resource estimate we consider preparing the function $\tanh(\bar{x})$. This function is, e.g., used as a sigmoid activation function in neural networks [46]. We consider the range $\bar{x} \in [0, 1]$ on $n = 32$ qubits, with the corresponding quantum state

$$|\Psi_{\tanh}\rangle = \frac{1}{\mathcal{N}_{\tanh}} \sum_{x=0}^{N-1} \tanh(\bar{x})|x\rangle. \quad (15)$$

We contrast our QET-based method with the state-of-the-art black-box method of [15], and the GR method [17], implementing all required amplitude oracles using the piecewise-polynomial approach [22]. The resources required by each of the three methods are shown in Table II.

Method	# Additional ancilla qubits	# Toffoli gates
QET-based (This work)	3	9.7×10^4
Black-box state preparation [15]	216	6.9×10^4
Grover-Rudolph [17]	> 959	> 2.0×10^5

TABLE II. Comparing the resources to generate a quantum state representing $\tanh(x)$ in the range $x \in [0, 1]$ on $n = 32$ qubits using our QET-based method, black-box state preparation [15] and the Grover-Rudolph method [17] (both using piecewise-polynomial amplitude oracles [22]). For the GR method, we minimize the number of calls to the amplitude oracle, which increases the number of ancilla qubits used. The reduction from 4 to 3 ancilla qubits for the QET-based method is due to the use of an approximating polynomial of definite parity.

QET-based approach. To apply our method, we approximate the composite function $h(y) = \tanh(\arcsin(y))$ with a degree $d = 33$ Taylor expansion, yielding an L_∞ error $< 10^{-7}$. As the Taylor expansion has odd parity, we require only a single QET ancilla (the gate complexity can be improved by a factor of around 1.5 using the $d = 10$ mixed-parity minimax polynomial, at the expense of an additional ancilla qubit). Using the analysis in Appendix B 1, the trace distance between the output and desired states is 10^{-6} (for $y \in [0, \sin(1)]$).

As N is large, we approximate $\mathcal{F}_{\bar{f}}^{[N]}$ by $\mathcal{F}_{\bar{f}}^{[\infty]} \approx 0.64$, which introduces a small probability of failure that we neglect here. As discussed in Appendix A we use an additional ancilla qubit to adjust the amplitude of the desired state to 0.5. We then require a single round of amplitude amplification, $R = 1$ (i.e. 2 calls to $U_{\bar{f}}$ and 1 call to $U_{\bar{f}}^\dagger$). We also require one Toffoli gate (for reflection around the good state), one $(n + 2)$ -controlled-NOT gate (for reflection around the initial state), and 3 R_y gates. A k -controlled-NOT can be implemented using $\mathcal{O}(k)$ CNOT and single-qubit gates, which can be tightened to $\approx 16k$ Toffoli gates if a spare dirty qubit can be used [47] — we assume access to such a borrowable qubit and use the latter upper bound in the following. As shown in Fig. 1b, each application of $U_{\bar{f}}, U_{\bar{f}}^{-1}$ requires $d/2$ applications of U_{\sin} and of U_{\sin}^\dagger , $2d$ CNOT gates, and d single-qubit rotations (the reduction in resources is a result of implementing a definite parity function). From Fig. 1a, each application of $U_{\sin}/U_{\sin}^\dagger$ requires n controlled- R_y gates (which can each be implemented with 2 single-qubit- R_y gates). Overall we require

$$(2R+1)(1+d(2n+1)) \text{ Rots} + R(16(n+2)+1) \text{ Toffs} \quad (16)$$

Using a typical estimate of 30 T gates per rotation, and an architecture that distills Toffoli gates and converts them to T gates (at a rate of 2 Ts per Toffoli [48]), we require approximately 9.7×10^4 Toffoli gates. We use three ancilla qubits; one to block-encode $\sin(x/N)$, one to implement QET, and one for exact amplitude amplification.

Black-box approach. To simplify the analysis of black-box state preparation, we only count non-Clifford gates due to the amplitude oracle, as these are the dominant contribution to the cost. Each round of amplitude amplification (again $R = 1$) uses the oracle and its inverse once, as well as one final application of the inverse once the state has been prepared [14]. Using Table II of [22], the amplitude oracle requires 23095 Toffoli gates (assuming an L_∞ error $< 10^{-7}$ is sufficient to obtain a trace distance $< 10^{-6}$). Hence, we require at least 6.9×10^4 Toffoli gates. The amplitude oracle requires 206 ancilla qubits⁵, and the implementation requires an additional $2 \log(n) - 1 = 9$ ancilla qubits [15], and we need 1 additional qubit for exact amplitude amplification.

Grover-Rudolph approach. For the GR method, we must coherently evaluate

$$\arcsin \left(\sqrt{\frac{\int_a^b \tanh^2(\bar{x})}{\int_c^d \tanh^2(\bar{x})}} \right), \quad (17)$$

using $\int \tanh^2(\bar{x}) = \bar{x} - \tanh(\bar{x})$, in each iteration. We lower bound the cost of this method by the cost of its

⁵ The qubit counts in Table II of [22] are missing one qubit.

final iteration. Using the minimal number of uncomputations, we require 4 evaluations of \tanh and one evaluation of \arcsin (and their uncomputations). From Table II of [22] this yields $(8 \times 23095) + (2 \times 7784) = 2.0 \times 10^5$ Toffoli gates. In addition, we must store all intermediate working registers, which requires at least $(4 \times 206) + 135 = 959$ ancilla qubits [22]. If we instead minimize the number of ancilla qubits used, we would require approximately $\max(206, 135) + 32 = 238$ ancilla qubits (enough for the largest garbage register and a 2nd main register to erase computed values), but would require a larger number of calls to the amplitude oracles, in order to make the computation reversible.

Quantitative analysis. We see from Table II that our approach requires $72 \times$ fewer logical ancilla qubits than black-box state preparation, while requiring only $1.4 \times$ more Toffoli gates. As discussed previously, this small footprint will be crucial in the early fault-tolerant era, where computations are constrained by space. Although the GR method has a complexity independent of $\mathcal{F}_{\bar{f}}^{[N]}$, we see that this is outweighed here by the large constant factors associated with coherently performing the integration.

V. EXTENSIONS

Non-smooth functions. We can extend our method to efficiently prepare functions with a modest number of discontinuities, which are typically pathological for QET/QSVT-based methods. Our application to state preparation enables us to circumvent this issue using two possible techniques.

The first route uses a coherent inequality test, using n Toffoli gates and n ancilla qubits, to entangle the register with a flag qubit (such that the flag qubit is $|0\rangle/|1\rangle$ for x to the left/right of the discontinuity). We control the rotations of the QET-ancilla on the flag, applying a different QET polynomial to each part of the register. For k discontinuities, this piecewise extension requires $(k+n)$ ancilla qubits and $2kn$ Toffoli gates for the inequality comparison (and its uncomputation), and replaces the singly-controlled rotations of the ancilla by k doubly-controlled rotations.

The second route is more resource efficient when the number of discontinuities is small. Take for example preparation of the triangle/tent-like function ($\bar{x} \in [0, 1]$)

$$f(\bar{x}) = \begin{cases} \bar{x} & 0 \leq \bar{x} \leq 1/3 \\ \frac{1}{2}(1 - \bar{x}) & 1/3 < \bar{x} \leq 1 \end{cases} \quad (18)$$

We can instead consider block encoding a continuously differentiable function that approximates ($\bar{x} \in [0, 7/3]$)

$$\bar{f}(\bar{x}) = \begin{cases} \bar{x} & 0 \leq \bar{x} \leq \frac{1}{3} \\ \text{Unspecified} & \frac{1}{3} < \bar{x} < 2 \\ \frac{1}{2}(\frac{7}{3} - \bar{x}) & 2 \leq \bar{x} \leq \frac{7}{3} \end{cases} \quad (19)$$

We analyze the case $n = 2$ to simplify the presentation. We implement a block-encoding of $\sum_x \bar{f}(\bar{x})|x\rangle\langle x|$ on $n+1 = 3$ qubits. The new range is $\bar{x} \in [0, \alpha]$, with $\alpha = \frac{2^{n+1}-1}{2^n-1} = \frac{7}{3}$, which ensures that $\bar{x} = \frac{\alpha x}{2^{n+1}-1} = \frac{x}{2^n-1} = \frac{x}{3}$. We then prepare an initial state $\frac{1}{2} \sum_{x=0}^3 |0\rangle|x\rangle$, and use a coherent inequality test to flip the ancilla qubit for $|x; \bar{x} > \frac{1}{3}\rangle$. This gives the state $\frac{1}{2}(|\mathbf{0}\rangle_3 + |\mathbf{1}\rangle_3 + |\mathbf{6}\rangle_3 + |\mathbf{7}\rangle_3)$ where $|\mathbf{i}\rangle_j$ denotes integer i encoded as a j -bit string. We apply the block-encoding of $\bar{f}(\bar{x})$ to this state, giving after amplitude amplification:

$$\frac{1}{2} \left(\bar{f}(0)|\mathbf{0}\rangle_3 + \bar{f}\left(\frac{1}{3}\right)|\mathbf{1}\rangle_3 + \bar{f}(2)|\mathbf{6}\rangle_3 + \bar{f}\left(\frac{7}{3}\right)|\mathbf{7}\rangle_3 \right). \quad (20)$$

We then reverse the earlier inequality check, and use that $f(\bar{x}) = \bar{f}(\bar{x} + \frac{4}{3})$ for $2 \leq \bar{x} \leq \frac{7}{3}$, to yield the desired state. In exchange for the added complexity of block-encoding the function in wider range, we can replace the non-analytic function $f(\bar{x})$ with a continuously differentiable function approximating $\bar{f}(\bar{x})$, requiring a substantially lower degree polynomial to approximate.

Priors. We can incorporate the use of improved priors in our method (cf. [18]). By applying $U_{\bar{f}}$ to $|+\rangle^{\otimes n}$, we are choosing a uniform prior, leading to the $1/\mathcal{F}_{\bar{f}}^{[N]}$ rounds of amplitude amplification. We can instead prepare $\mathcal{N}_p^{-1} \sum_x p(\bar{x})|x\rangle|000\rangle$ and block-encode a polynomial approximation of $f(\bar{x})/p(\bar{x})$. We require $\mathcal{O}\left(\mathcal{N}_f^{-1} \mathcal{N}_p |f/p|_{\max}\right)$ rounds of amplitude amplification. If the prior distribution can be prepared with low cost, has a similar normalisation to $f(\bar{x})$, and there exists a similar degree approximation of $f(\bar{x})/p(\bar{x})$ as there is for $f(\bar{x})$, this can reduce the resources required to prepare the desired function.

Fourier series. Our method is naturally compatible with ‘Fourier-based QET’ [27, 49] which provides a complementary approach for function approximation through Fourier series. In that approach, the block-encoding of A is replaced by controlled time evolution $U(A) := |0\rangle\langle 0| \otimes I + |1\rangle\langle 1| \otimes e^{iAt}$. We can implement $U(A)$ for diagonal $A = \sum_x \bar{x}|x\rangle\langle x|$ using n controlled-Z rotations. Fourier-based QET uses repeated calls to $U(A)$, together with single-qubit-rotations, to apply a function expressed as a Fourier series to the eigenvalues of A . Our methods are particularly appealing for functions with a compact Fourier series, such as spherical harmonic functions used in quantum chemistry [11, 12].

Cycloid function. We present an example demonstrating the utility of Fourier-QET. We consider implementing the cycloid function (a cycloid is the shape traced out by a point on a circle rolling in the $X - Y$ plane). It does not have a clean functional form; $y(x) = \frac{1}{2}(1 - \cos(\phi(x)))$ with $\phi(x)$ the functional inverse of $(x - \sin(x))$. However, the function can be described by its (even) Fourier series. For an ($n = 32$)-bit approximation of the cycloid function in the range $\bar{x} \in [0, 2\pi]$, we find that a $d = 120$ Fourier series is suf-

ficient to approximate the function within an L_2 error of $< 10^{-3}$. The Fourier-QET method requires d applications each of $U(A), U(A)^\dagger$, and $8d + 4$ single-qubit rotations [49]. Each application of $U(A), U(A)^\dagger$ requires n controlled- R_z gates, which can each be implemented using 2 single-qubit- R_z rotations. Overall, we require $4(d(n + 2) + 1)$ single-qubit-rotations, which we approximate as $60d(n + 2)$ Toffoli gates, to block-encode the Fourier series. The filling-fraction $\mathcal{F}_f^{[\infty]}$ is approximately 0.79, so we can use $R = 1$ round of exact amplitude amplification (which adds 1 qubit). Overall we require roughly

$$[60d(n + 2)(2R + 1) + 16(n + 1)R] \approx 7.35 \times 10^5 \quad (21)$$

Toffoli gates and 2 ancilla qubits to prepare the desired state. It is not obvious how to prepare this function using the black-box or GR approaches, as we cannot define closed forms of the function or its integral (away from nodal points), rendering a coherent arithmetic-based amplitude oracle non-trivial.

VI. OUTLOOK

Conclusion. We have introduced a QET-based approach to preparing quantum states that represent continuous functions with polynomial or Fourier series approximations. By circumventing the coherent arithmetic instantiated amplitude oracle typically used, we can significantly reduce the number of ancilla qubits required. Our approach enables the same circuit template to be used for all suitable functions, in contrast to the bespoke circuits typically developed for different functions' amplitude oracles. We have illustrated how to use our methods for preparing Gaussian, Kaiser window, tanh and cycloid functions with lower complexity than prior state-of-the-art approaches.

Scope. We expect our technique to prove useful in a wide range of quantum algorithms, including those for chemistry and physics simulation, finance, phase estimation, and differential equation solving. One current drawback of our method is that it cannot efficiently prepare the state representing $\sqrt{\bar{x}}$ for $\bar{x} \in [0, 1]$, which is

often used to calculate payoffs in quantum algorithms for derivative pricing [8, 9]. Because the function is non-differentiable at $\bar{x} = 0$, we cannot formulate a Taylor expansion around this point. Moreover, because the function is non-periodic, and has a large discontinuity, its Fourier series has a large error at the interval edges due to the Gibbs phenomenon. One possible solution is to consider the function away from 0 (e.g. $\sqrt{\bar{x} + a}$). However, if this is not suitable in the desired application, then alternative solutions will need to be developed.

Multivariate functions. A straightforward extension of our approach to multivariate functions is to introduce additional register qubits $\sum_{x,y} |x\rangle|y\rangle$, and use linear combinations of block-encodings (LCBE) and products of block-encodings (PBE) [31] to implement a function $f(x, y)$ with a series expansion in powers of x, y . Each invocation of LCBE requires an additional ancilla qubit and reduces the normalization of the block-encoded function by a factor of two. The expansion coefficients (which determine the final normalization of the block-encoding) can be much smaller in the Fourier basis than in the polynomial basis, which reduces the number of rounds of amplitude amplification required. A potentially more efficient route to generate a multivariate function $f(\vec{x})$ may be to use the recently introduced multivariable-QSP [50], which can be lifted to multivariable-QSVT for commuting block-encoded operators (as is the case here). Nevertheless, characterizing the functions that can be implemented via M-QSP is still an ongoing area of research. Another route towards implementing multivariate functions would be to lift the single-qubit quantum Universal Approximation Theorem from [51] (which shows that a sequence of single-qubit rotations can approximate any multivariate continuous function in the same way as classical neural networks can) to the commuting multi-qubit operator case, taking inspiration from analogous lifts from QSP [28] to QET/QSVT [31], and Fourier-QSP [51] to Fourier-QET [49].

Acknowledgements. We thank Fernando Brandão for discussions and support throughout the project. A.G. acknowledges funding from the AWS Center for Quantum Computing.

-
- [1] A. Montanaro and S. Pallister, *Physical Review A* **93**, 032324 (2016).
 - [2] A. Scherer, B. Valiron, S.-C. Mau, S. Alexander, E. Van den Berg, and T. E. Chapuran, *Quantum Information Processing* **16**, 1 (2017).
 - [3] D. W. Berry, A. M. Childs, A. Ostrander, and G. Wang, *Communications in Mathematical Physics* **356**, 1057 (2017).
 - [4] S. K. Leyton and T. J. Osborne, arXiv preprint arXiv:0812.4423 (2008).
 - [5] Y. Cao, A. Papageorgiou, I. Petras, J. Traub, and S. Kais, *New Journal of Physics* **15**, 013021 (2013).
 - [6] S. P. Jordan, K. S. Lee, and J. Preskill, *Science* **336**, 1130 (2012).
 - [7] N. Kleo and M. J. Savage, *Phys. Rev. A* **104**, 062425 (2021).
 - [8] N. Stamatopoulos, D. J. Egger, Y. Sun, C. Zoufal, R. Iten, N. Shen, and S. Woerner, *Quantum* **4**, 291 (2020).
 - [9] S. Chakrabarti, R. Krishnakumar, G. Mazzola, N. Stamatopoulos, S. Woerner, and W. J. Zeng,

- [Quantum 5, 463 \(2021\)](#).
- [10] D. W. Berry, Y. Su, C. Gyurik, R. King, J. Basso, A. D. T. Barba, A. Rajput, N. Wiebe, V. Dunjko, and R. Babbush, arXiv preprint arXiv:2209.13581 (2022).
- [11] N. J. Ward, I. Kassal, and A. Aspuru-Guzik, *The Journal of Chemical Physics* **130**, 194105 (2009).
- [12] H. H. S. Chan, R. Meister, T. Jones, D. P. Tew, and S. C. Benjamin, arXiv preprint arXiv:2202.05864 (2022).
- [13] L. K. Grover, *Physical Review Letters* **85**, 1334 (2000).
- [14] Y. R. Sanders, G. H. Low, A. Scherer, and D. W. Berry, *Physical Review Letters* **122**, 020502 (2019).
- [15] S. Wang, Z. Wang, G. Cui, S. Shi, R. Shang, L. Fan, W. Li, Z. Wei, and Y. Gu, *Quantum Information Processing* **20**, 1 (2021).
- [16] A. G. Rattew and B. Koczor, arXiv preprint arXiv:2205.00519 (2022).
- [17] L. Grover and T. Rudolph, arXiv preprint quant-ph/0208112 (2002).
- [18] J. Bausch, *Quantum* **6** (2022).
- [19] S. Wang, Z. Wang, R. He, G. Cui, S. Shi, R. Shang, J. Li, Y. Li, W. Li, Z. Wei, *et al.*, *New Journal of Physics* **24**, 103004 (2022).
- [20] E. Muñoz-Coreas and H. Thapliyal, *ACM Journal on Emerging Technologies in Computing Systems (JETC)* **14**, 1 (2018).
- [21] M. K. Bhaskar, S. Hadfield, A. Papageorgiou, and I. Petras, *Quantum Information and Computation* **16** (2016).
- [22] T. Häner, M. Roetteler, and K. M. Svore, arXiv preprint arXiv:1805.12445 (2018).
- [23] “Scirate thread on state preparation,” <https://scirate.com/arxiv/2205.00519> (2022), accessed: 2022-08-05.
- [24] E. T. Campbell, *Quantum Science and Technology* **7**, 015007 (2021).
- [25] K. Wan, M. Berta, and E. T. Campbell, *Physical Review Letters* **129**, 030503 (2022).
- [26] L. Lin and Y. Tong, [PRX Quantum 3, 010318 \(2022\)](#).
- [27] Y. Dong, L. Lin, and Y. Tong, arXiv preprint arXiv:2204.05955 (2022).
- [28] G. H. Low, T. J. Yoder, and I. L. Chuang, *Physical Review X* **6**, 041067 (2016).
- [29] G. H. Low and I. L. Chuang, [Physical Review Letters 118, 010501 \(2017\)](#).
- [30] G. H. Low and I. L. Chuang, [Quantum 3, 163 \(2019\)](#).
- [31] A. Gilyén, Y. Su, G. H. Low, and N. Wiebe, in *Proceedings of the 51st Annual ACM SIGACT Symposium on Theory of Computing*, STOC 2019 (2019) pp. 193–204.
- [32] J. M. Martyn, Z. M. Rossi, A. K. Tan, and I. L. Chuang, *PRX Quantum* **2**, 040203 (2021).
- [33] Y. Dong, X. Meng, K. B. Whaley, and L. Lin, *Physical Review A* **103**, 042419 (2021).
- [34] E. Y. Remez, *General computational methods of Chebyshev approximation: The problems with linear real parameters* (US Atomic Energy Commission, Division of Technical Information, 1962).
- [35] W. Fraser, *Journal of the ACM* **12**, 295 (1965).
- [36] R. Chao, D. Ding, A. Gilyen, C. Huang, and M. Szegedy, arXiv preprint arXiv:2003.02831 (2020).
- [37] J. Haah, [Quantum 3, 190 \(2019\)](#).
- [38] J. J. García-Ripoll, *Quantum* **5**, 431 (2021).
- [39] A. Holmes and A. Matsuura, in *2020 IEEE International Conference on Quantum Computing and Engineering* (2020) pp. 169–179.
- [40] P. Rall, [Quantum 5, 566 \(2021\)](#).
- [41] I. D. Kivlichan, N. Wiebe, R. Babbush, and A. Aspuru-Guzik, *Journal of Physics A: Mathematical and Theoretical* **50**, 305301 (2017).
- [42] A. Kitaev and W. A. Webb, arXiv preprint arXiv:0801.0342 (2008).
- [43] C. W. Bauer, P. Deliyannis, M. Freytsis, and B. Nachman, arXiv preprint arXiv:2109.10918 (2021).
- [44] N. Klco and M. J. Savage, [Phys. Rev. A 102, 012612 \(2020\)](#).
- [45] A. G. Rattew, Y. Sun, P. Minssen, and M. Pistoia, [Quantum 5, 609 \(2021\)](#).
- [46] B. L. Kalman and S. C. Kwasny, in *Proceedings 1992 IJCNN International Joint Conference on Neural Networks*, Vol. 4 (1992) pp. 578–581.
- [47] C. Gidney, “Constructing large controlled-nots,” <https://algassert.com/circuits/2015/06/05/Constructing-Large> (2015), accessed: 2022-08-05.
- [48] C. Gidney and A. G. Fowler, *Quantum* **3**, 135 (2019).
- [49] T. d. L. Silva, L. Borges, and L. Aolita, arXiv preprint arXiv:2206.02826 (2022).
- [50] Z. M. Rossi and I. L. Chuang, *Quantum* **6**, 811 (2022).
- [51] A. Pérez-Salinas, D. López-Núñez, A. García-Sáez, P. Forn-Díaz, and J. I. Latorre, *Physical Review A* **104**, 012405 (2021).
- [52] A. Grinshpan, “[Analysis notes](#),” (2009).
- [53] M. Abramowitz and I. A. Stegun, *Handbook of Mathematical Functions, with Formulas, Graphs, and M* (Dover Publications Inc., New York, NY, USA, 1974).
- [54] J. van Apeldoorn, A. Gilyén, S. Gribling, and R. de Wolf, [Quantum 4, 230 \(2020\)](#), earlier version in FOCS’17. arXiv:1705.01843.

Appendix A: Exact amplitude amplification

In this appendix we describe exact amplitude amplification. This result is folklore, but we could not find a standard reference, especially one that treats the case when the amplitude is only approximately known, so we give a full treatment here.

We utilize Chebyshev polynomials of the first kind defined as $T_n(x) = \cos(n \arccos(x))$, and their recurrence relation $T_{n+1}(x) = 2xT_n(x) - T_{n-1}(x)$.

Lemma 1 (Amplitude amplification). *Let U be an n -qubit unitary, Π an n -qubit projector, $|\psi\rangle$ an n -qubit (normalized) quantum state, and $a \geq 0$ such that*

$$\Pi U |\bar{0}\rangle = a |\psi\rangle, \quad (\text{A1})$$

where $|\bar{0}\rangle$ denotes some n -qubit initial state.

Let $W = U(2|\bar{0}\rangle\langle\bar{0}| - I)U^\dagger(2\Pi - I)$, then

$$\Pi W^k U |\bar{0}\rangle = T_{2k+1}(a) |\psi\rangle, \quad \text{and} \quad (\text{A2})$$

$$\langle\bar{0}| U^\dagger (2\Pi - I) W^k U |\bar{0}\rangle = T_{2k+2}(a). \quad (\text{A3})$$

Proof. Equations (A2) and (A3) follow for $k = 0$ from (A1) using that $T_1(x) = x$ and $T_2(x) = 2x^2 - 1$.

We prove them for positive values of k by induction:

$$\begin{aligned}
\Pi W^{k+1} U |\bar{0}\rangle &= \Pi U (2|\bar{0}\rangle\langle\bar{0}| - I) U^\dagger (2\Pi - I) W^k U |\bar{0}\rangle \\
&= (2a|\psi\rangle\langle\bar{0}| - \Pi U) U^\dagger (2\Pi - I) W^k U |\bar{0}\rangle \\
&= 2a|\psi\rangle\langle\bar{0}| U^\dagger (2\Pi - I) W^k U |\bar{0}\rangle - \Pi W^k U |\bar{0}\rangle \\
&= (2aT_{2k+2}(a) - T_{2k+1}(a)) |\psi\rangle \\
&= T_{2k+3}(a) |\psi\rangle,
\end{aligned}$$

and

$$\begin{aligned}
\langle\bar{0}| U^\dagger (2\Pi - I) W^{k+1} U |\bar{0}\rangle &= 2\langle\bar{0}| U^\dagger \Pi W^{k+1} U |\bar{0}\rangle - \langle\bar{0}| U^\dagger W^{k+1} U |\bar{0}\rangle \\
&= 2\langle\bar{0}| U^\dagger \Pi W^{k+1} U |\bar{0}\rangle - \langle\bar{0}| U^\dagger W^{k+1} U |\bar{0}\rangle \\
&= 2aT_{2k+3}(a) - \langle\bar{0}| U^\dagger W^{k+1} U |\bar{0}\rangle \\
&= 2aT_{2k+3}(a) - \langle\bar{0}| U^\dagger U (2|\bar{0}\rangle\langle\bar{0}| - I) U^\dagger (2\Pi - I) W^k U |\bar{0}\rangle \\
&= 2aT_{2k+3}(a) - \langle\bar{0}| U^\dagger (2\Pi - I) W^k U |\bar{0}\rangle \\
&= 2aT_{2k+3}(a) - T_{2k+2}(a) \\
&= T_{2k+4}(a).
\end{aligned}$$

Theorem 4 (Exact amplitude amplification). *Suppose U , Π , $|\psi\rangle$, $|\bar{0}\rangle$, and a are as in Lemma 1. Let $k := \left\lceil \frac{\pi}{4\arcsin(a)} - \frac{1}{2} \right\rceil$, and let $\theta := \frac{\pi}{4k+2}$. Suppose that R is a single-qubit unitary such that $\langle 0|R|0\rangle = \frac{\sin(\theta)}{a}$. Let us define $U' := R \otimes U$ and*

$$W' := U' (2|0\rangle\langle 0| \otimes |\bar{0}\rangle\langle\bar{0}| - I) U^\dagger (I - 2|0\rangle\langle 0| \otimes \Pi),$$

then

$$(W')^k U' |0\rangle |\bar{0}\rangle = |0\rangle |\psi\rangle. \quad (\text{A4})$$

Moreover, if $\tilde{a} \leq 2a < 2$ and \tilde{U} is such that

$$\Pi \tilde{U} |\bar{0}\rangle = \tilde{a} |\tilde{\psi}\rangle, \quad (\text{A5})$$

then

$$(|0\rangle\langle 0| \otimes \Pi) (\tilde{W}')^k (R \otimes \tilde{U}) |0\rangle |\bar{0}\rangle = c |0\rangle |\tilde{\psi}\rangle, \quad (\text{A6})$$

for some $c \geq 1 - (2k+1)(2k+2)|\tilde{a} - a|^2$, where \tilde{W}' is defined analogously to W' just U' is replaced by $R \otimes \tilde{U}$.

Proof. First note that

$$\theta = \frac{\pi}{4\left[\frac{\pi}{4\arcsin(a)} - \frac{1}{2}\right] + 2} \leq \frac{\pi}{4\left(\frac{\pi}{4\arcsin(a)} - \frac{1}{2}\right) + 2} = \arcsin(a),$$

and therefore $\langle 0|R|0\rangle = \frac{\sin(\theta)}{a} \leq 1$. Observe that $(|0\rangle\langle 0| \otimes \Pi) U' |0\rangle |\bar{0}\rangle = (|0\rangle\langle 0| \otimes \Pi) (R \otimes U) |\bar{0}\rangle = \sin(\theta) |0\rangle |\psi\rangle$. Applying Lemma 1 with U' , $\Pi' := |0\rangle\langle 0| \otimes \Pi$, $|\psi'\rangle := |0\rangle |\psi\rangle$, $|\bar{0}'\rangle := |0\rangle |\bar{0}\rangle$, and $a' := \sin(\theta)$ we get that

$$\Pi' (-W')^k U' |\bar{0}'\rangle = T_{2k+1}(\sin(\theta)) |\psi'\rangle,$$

thus

$$\Pi' (W')^k U' |\bar{0}'\rangle = (-1)^k T_{2k+1}(\sin(\theta)) |\psi'\rangle = |\psi'\rangle,$$

where the last equality holds because

$$\begin{aligned}
(-1)^k T_{2k+1}(\sin(\theta)) &= (-1)^k \cos((2k+1) \arccos(\sin(\theta))) \\
&= (-1)^k \cos((2k+1)(\pi/2 - \theta)) \\
&= (-1)^k \cos(k\pi) = 1.
\end{aligned}$$

Similarly, by Lemma 1 we get that

$$\Pi' (\tilde{W}')^k (R \otimes \tilde{U}) |\bar{0}'\rangle = (-1)^k T_{2k+1}\left(\sin(\theta) \frac{\tilde{a}}{a}\right) |0\rangle |\tilde{\psi}\rangle.$$

As we have seen $(-1)^k T_{2k+1}(y)$ takes value 1 at $y = \sin(\theta)$, which also implies that its derivative is 0 there since $|T_{2k+1}(y)| \leq 1$ for all $y \in [-1, 1]$ and $\sin(\theta) < 1$ (as $a < 1$). By Taylor's theorem we have that $(-1)^k T_{2k+1}(\sin(\theta) + \xi) \geq 1 - \frac{M_2}{2} \xi^2$, where M_2 is the maximal absolute value of the second derivative of $T_{2k+1}(y)$ at any point between $\sin(\theta)$ and $\sin(\theta + \xi)$. Observe that $|\sin(\theta) \frac{\tilde{a}}{a} - \sin(\theta)| = \frac{\sin(\theta)}{a} |\tilde{a} - a| \leq |\tilde{a} - a|$ so in Taylor's theorem we can bound $|\xi| \leq |\tilde{a} - a|$.

If $\tilde{a} \leq 2a$ then $\max\{\sin(\theta), \sin(\theta) \frac{\tilde{a}}{a}\} \leq 2\sin(\theta)$, so it suffices to bound the magnitude of the second derivative $|T_{2k+1}''(y)|$ for $y \in [-2\sin(\theta), 2\sin(\theta)]$. If $a \in [\frac{1}{2}, 1]$, then $k = 1$ and $|T_3''(y)| = |24y| \leq 2(2k+1)(2k+2)$ so $M_2 \leq 2(2k+1)(2k+2)$. If $a \in [\sin(\pi/10), \frac{1}{2}]$, then $k = 2$ and $|T_5''(y)| = |320y^3 - 120y| \leq (2k+1)(2k+2)$ for $y \in [-2\sin(\pi/10), 2\sin(\pi/10)]$ so $M_2 \leq (2k+1)(2k+2)$. Finally, for $a < \sin(\pi/10)$ we have $k \geq 3$ and $2\sin(\theta) \leq 2\sin(\pi/14) < 0.45$. Considering $\alpha := n \arccos(y)$ and $y \in [-1, 1]$ we have $|T_n''(y)| = n \left| \frac{n \cos(\alpha) \sqrt{1-y^2} - y \sin(\alpha)}{(1-y^2)^{\frac{3}{2}}} \right| \leq \frac{n(n+1)}{(1-y^2)^{\frac{3}{2}}}$ which is $\leq 2n(n+1)$ for $y \in [-\frac{1}{2}, \frac{1}{2}]$. This completes the case separation and proves that $M_2/2 \leq (2k+1)(2k+2)$ implying that $c \geq 1 - (2k+1)(2k+2)|\tilde{a} - a|^2$. \square

As discussed in the main text, we use QET to implement $U_{\tilde{f}}$ a $(1, 3, 0)$ block-encoding of

$$\sum_{x=0}^{N-1} \frac{\tilde{f}(\bar{x})}{2|\tilde{f}(\bar{x})|_{\max}} |x\rangle \langle x|. \quad (\text{A7})$$

This leads to our heralded state-preparation unitary $U_{\tilde{f}} H^{\otimes n}$ such that

$$(I_n \otimes \langle \bar{0}|_3) U_{\tilde{f}} H^{\otimes n} (|\bar{0}\rangle_{n+3}) = \frac{\mathcal{F}_{\tilde{f}}^{[N]}}{2} |\Psi_{\tilde{f}}\rangle.$$

If we know the value of $\mathcal{F}_{\tilde{f}}^{[N]}$, then we can apply Theorem 4 to get the final unitary that prepares $|\Psi_{\tilde{f}}\rangle$ exactly. This keeps the number of required amplification rounds $\mathcal{O}\left(1/\mathcal{F}_{\tilde{f}}^{[N]}\right)$ and only introduces a single additional ancilla qubit.⁶ The gate R therein can be chosen for example as a Y rotation $R_y(\phi)$ with angle $2 \arccos(\sin(\theta)/a)$.

⁶ For the implementation of the generalized Toffoli required for the reflection around the all-0 initial state we might need an additional second ancilla qubit.

1. Working with approximately known amplitudes

We discuss how best to amplify the state in cases where we do not know the exact value of $\mathcal{F}_{\tilde{f}}^{[N]}$. This may arise because the value n is so large that it would be too costly to classically compute the filling fraction. If we have a lower bound for $\mathcal{F}_{\tilde{f}}^{[N]}$, then we can simply apply fixed-point amplitude amplification, using QSVT [31]. This also only uses a single additional ancilla qubit⁶ and increases the success probability to $\geq (1 - \zeta)$ at the cost of a multiplicative overhead of $\mathcal{O}(\log(\zeta^{-1}))$.

If n is sufficiently large, it is possible to approximate the value of $\mathcal{F}_{\tilde{f}}^{[N]}$ by its continuous counterpart $\mathcal{F}_{\tilde{f}}^{[\infty]}$ or $\mathcal{F}_f^{[\infty]}$, c.f. Appendix A 2, which is efficient to evaluate for many functions. Assuming that $|\mathcal{F}_{\tilde{f}}^{[\infty]} - \mathcal{F}_{\tilde{f}}^{[N]}| \leq \delta \leq \mathcal{F}_{\tilde{f}}^{[\infty]}$, we can apply Theorem 4 for bounding the error in the resulting amplitude by

$$\mathcal{O}\left(\left(\frac{\delta}{\mathcal{F}_{\tilde{f}}^{[\infty]}}\right)^2\right).$$

As the approximation error δ decreases exponentially with the number of qubits n used for discretizing the function, we expect this error to be small.

2. General discretization error bounds

Here we recall some standard results on Riemann sums. The first result considers our default discretization method but has a looser bound, while the second improves upon the first bound but requires a slightly different placing of the discrete points.

Lemma 2 (see [52]). *Suppose that $f: [a, b] \rightarrow \mathbb{R}$ is continuously differentiable. Let $\bar{x} = ((b - a)x/N + a)$, then*

$$\left| \frac{b-a}{N} \sum_{x=0}^{N-1} f(\bar{x}) - \int_a^b f(x) dx \right| \leq \frac{(b-a)^2}{2N} |f'(x)|_{\max}^{x \in [a, b]}.$$

Lemma 3 (see [52]). *Suppose that $f: [a, b] \rightarrow \mathbb{R}$ is twice continuously differentiable. Let $\bar{x} = ((b - a)(x + \frac{1}{2})/N + a)$, then*

$$\left| \frac{b-a}{N} \sum_{x=0}^{N-1} f(\bar{x}) - \int_a^b f(x) dx \right| \leq \frac{(b-a)^3}{24N^2} |f''(x)|_{\max}^{x \in [a, b]}.$$

Appendix B: Error analysis

In this Appendix we prove Theorem 1, which we restate below:

Theorem 1. *Given a polynomial of degree d_δ that (when applied to $\sin(x/N)$) approximates $f(\bar{x})/|f|_{\max}$ to L_∞ -error $\delta = \epsilon \cdot \text{Min}(\mathcal{F}_f^{[N]}, \mathcal{F}_{\tilde{f}}^{[N]})$, we can prepare a quantum state $|\Psi_{\tilde{f}}\rangle$ that is ϵ -close in trace-distance to $|\Psi_f\rangle$ using*

$$\mathcal{O}\left(\frac{n \cdot d_\delta}{\mathcal{F}_{\tilde{f}}^{[N]}}\right) \text{ gates.} \quad (10)$$

Proof. We first seek to bound the trace distance between the approximate state prepared $|\Psi_{\tilde{f}}\rangle$, and the desired state $|\Psi_f\rangle$. The error in the polynomial approximation determines this trace distance. As we can apply amplitude amplification appropriately for the implemented approximate polynomial, we can consider the trace distance obtained conditioned on amplitude amplification succeeding. As in the main text, $\mathcal{N}_f = \sqrt{\sum_x |f(\bar{x})|^2}$.

We first define scaled versions of f and \tilde{f} , defined here as h and \tilde{h} respectively, such that $|h|_{\max}, |\tilde{h}|_{\max} \leq 1$. We construct our degree d polynomial approximation such that

$$|h - \tilde{h}|_{\max} \leq \delta. \quad (B1)$$

This implies

$$h\tilde{h} \geq \frac{1}{2}(h^2 + \tilde{h}^2 - \delta^2). \quad (B2)$$

The trace distance between the states is

$$D(|\Psi_{\tilde{f}}\rangle, |\Psi_f\rangle) = D(|\Psi_{\tilde{h}}\rangle, |\Psi_h\rangle) \quad (B3)$$

$$= \sqrt{1 - |\langle \Psi_h | \Psi_{\tilde{h}} \rangle|^2}. \quad (B4)$$

We focus on $|\langle \Psi_h | \Psi_{\tilde{h}} \rangle|^2$, and use the above bound on $h\tilde{h}$

$$|\langle \Psi_h | \Psi_{\tilde{h}} \rangle|^2 = \left| \frac{1}{\mathcal{N}_h \mathcal{N}_{\tilde{h}}} \sum_x h(\bar{x}) \tilde{h}(\bar{x}) \right|^2 \quad (B5)$$

$$\geq \left| \frac{1}{2\mathcal{N}_h \mathcal{N}_{\tilde{h}}} \sum_x |h(\bar{x})|^2 + |\tilde{h}(\bar{x})|^2 - \delta^2 \right|^2 \quad (B6)$$

$$= \frac{1}{4} \left| \frac{\mathcal{N}_h}{\mathcal{N}_{\tilde{h}}} + \frac{\mathcal{N}_{\tilde{h}}}{\mathcal{N}_h} - \frac{N\delta^2}{\mathcal{N}_{\tilde{h}} \mathcal{N}_h} \right|^2 \quad (B7)$$

We expand out the square to give

$$\frac{1}{4} \left(\frac{\mathcal{N}_h^2}{\mathcal{N}_{\tilde{h}}^2} + \frac{\mathcal{N}_{\tilde{h}}^2}{\mathcal{N}_h^2} + 2 - \frac{2N\delta^2}{\mathcal{N}_{\tilde{h}} \mathcal{N}_h} \left(\frac{\mathcal{N}_h}{\mathcal{N}_{\tilde{h}}} + \frac{\mathcal{N}_{\tilde{h}}}{\mathcal{N}_h} \right) + \left(\frac{N\delta^2}{\mathcal{N}_{\tilde{h}} \mathcal{N}_h} \right)^2 \right) \quad (B8)$$

We then let $\mathcal{N}_h = A$ and $\mathcal{N}_{\tilde{h}} = B$ in the first two terms. We can use

$$\frac{A^2}{B^2} + \frac{B^2}{A^2} \geq 2 \quad (B9)$$

(as $(A^2 - B^2) \geq 0$) to simplify the above expression to

$$\geq \frac{1}{4} \left(4 - \frac{2N\delta^2}{\mathcal{N}_{\tilde{h}}\mathcal{N}_h} \left(\frac{\mathcal{N}_h}{\mathcal{N}_{\tilde{h}}} + \frac{\mathcal{N}_{\tilde{h}}}{\mathcal{N}_h} \right) + \left(\frac{N\delta^2}{\mathcal{N}_{\tilde{h}}\mathcal{N}_h} \right)^2 \right). \quad (\text{B10})$$

We can also drop the final term, as it strictly increases the value of the expression

$$\geq 1 - \frac{N\delta^2}{2\mathcal{N}_{\tilde{h}}\mathcal{N}_h} \left(\frac{\mathcal{N}_h}{\mathcal{N}_{\tilde{h}}} + \frac{\mathcal{N}_{\tilde{h}}}{\mathcal{N}_h} \right) \quad (\text{B11})$$

$$= 1 - \frac{N\delta^2}{2} \left(\frac{\mathcal{N}_h^2 + \mathcal{N}_{\tilde{h}}^2}{\mathcal{N}_{\tilde{h}}^2\mathcal{N}_h^2} \right) \quad (\text{B12})$$

We now define $\alpha = \text{Max}(\mathcal{N}_{\tilde{h}}, \mathcal{N}_h)$, $\beta = \text{Min}(\mathcal{N}_{\tilde{h}}, \mathcal{N}_h)$, such that $\alpha \geq \beta$ (thus $\beta^2/\alpha^2 \leq 1$). Then

$$\frac{\alpha^2 + \beta^2}{\alpha^2\beta^2} = \frac{\alpha^2 \left(1 + \frac{\beta^2}{\alpha^2} \right)}{\alpha^2\beta^2} \leq \frac{2}{\beta^2}. \quad (\text{B13})$$

Eq. (B12) then becomes $\geq 1 - \frac{N\delta^2}{\beta^2}$, with $\beta = \text{Min}(\mathcal{N}_{\tilde{h}}, \mathcal{N}_h)$. We now examine the value N/β^2 . Without loss of generality, choose $\beta = \mathcal{N}_h$ here. Then we have

$$\frac{N}{\mathcal{N}_h^2} = \frac{N|f|_{\text{max}}^2}{\mathcal{N}_f^2} = \left(\mathcal{F}_f^{[N]} \right)^{-2} \quad (\text{B14})$$

using the definition of the discretized L2-filling fraction from the main text. Hence

$$|\langle \Psi_h | \Psi_{\tilde{h}} \rangle|^2 \geq 1 - \left(\frac{\delta}{\text{Min}(\mathcal{F}_f^{[N]}, \mathcal{F}_{\tilde{f}}^{[N]})} \right)^2 \quad (\text{B15})$$

As a result, we find

$$D(|\Psi_{\tilde{f}}\rangle, |\Psi_f\rangle) \leq \frac{\delta}{\text{Min}(\mathcal{F}_f^{[N]}, \mathcal{F}_{\tilde{f}}^{[N]})}. \quad (\text{B16})$$

To achieve a trace distance of ϵ in the state, we therefore must approximate the polynomial to a factor of

$$\delta = \epsilon \cdot \text{Min}(\mathcal{F}_f^{[N]}, \mathcal{F}_{\tilde{f}}^{[N]}). \quad (\text{B17})$$

As discussed in Appendix A, we can use exact amplitude amplification to implement a $(1, 4, 0)$ block-encoding of $|\Psi_{\tilde{f}}\rangle\langle\tilde{0}|$, that makes $\mathcal{O}(1/\mathcal{F}_{\tilde{f}}^{[N]})$ calls to $U_{\tilde{f}}$, $U_{\tilde{f}}^\dagger$, and a similar number of $(n+4)$ -qubit (anti)-controlled-Z gates, 4-qubit (anti)-controlled-Z gates, Hadamard transform $H^{\otimes n}$ and R_y gates. $U_{\tilde{f}}$, $U_{\tilde{f}}^\dagger$ each make $d_\delta/2$ calls to U_{sin} and to U_{sin}^\dagger , and use a similar number of CNOT, singly-controlled R_z , and Hadamard gates. U_{sin} , U_{sin}^\dagger each use $\mathcal{O}(n)$ R_y gates, and an X gate.

The circuit thus requires $\mathcal{O}\left(\frac{nd_\delta}{\mathcal{F}_{\tilde{f}}^{[N]}}\right)$ gates to block-encode the state preparation matrix $|\Psi_{\tilde{f}}\rangle\langle\tilde{0}|$, which prepares $|\Psi_{\tilde{f}}\rangle$, an ϵ -accurate approximation to $|\Psi\rangle$ when $\delta = \epsilon \cdot \text{Min}(\mathcal{F}_f^{[N]}, \mathcal{F}_{\tilde{f}}^{[N]})$. \square

1. Error analysis in practice

The above analysis is an overly pessimistic error bound, as it assumes that the error in the function approximation is the same at every point. For approximation methods such a Taylor series, the maximum error can be considerably larger than the average error. As a result, we can directly calculate the trace distance between the states

$$\begin{aligned} D(|\Psi_{\tilde{f}}\rangle, |\Psi_f\rangle) &= \sqrt{1 - |\langle \Psi_f | \Psi_{\tilde{f}} \rangle|^2} \quad (\text{B18}) \\ &= \sqrt{1 - \left| \sum_x \frac{f(\bar{x})\tilde{f}(\bar{x})}{\mathcal{N}_f \cdot \mathcal{N}_{\tilde{f}}} \right|^2}. \end{aligned}$$

For a sufficiently large number of discretization points

$$\int_a^b y(\bar{x})d\bar{x} \approx \frac{(b-a)}{N} \sum_{x=0}^{N-1} y(\bar{x}), \quad (\text{B19})$$

as shown in Appendix A 2, which lets us approximate the trace distance between the states by

$$\sqrt{1 - \left| \frac{\int_a^b f(\bar{x})\tilde{f}(\bar{x})d\bar{x}}{\|f\|_2 \cdot \|\tilde{f}\|_2} \right|^2}. \quad (\text{B20})$$

Appendix C: Modified Bessel functions

In this appendix we list some properties of modified Bessel functions that we use later for analyzing Kaiser Windows. First let us recall [53, Eq. (9.6.12)] the Taylor series of $I_0(z)$:

$$I_0(z) = \sum_{k=0}^{\infty} \frac{(z^2/4)^k}{(k!)^2}. \quad (\text{C1})$$

We will also use the following integral representations [53, Eqs. (9.6.18-9.6.19)]:

$$I_n(z) = \frac{1}{\pi} \int_0^\pi \exp(z \cos(\theta)) \cos(n\theta) d\theta \quad (\text{C2})$$

$$= \frac{\left(\frac{z}{2}\right)^n}{\sqrt{\pi}\Gamma(n + \frac{1}{2})} \int_0^\pi \exp(z \cos(\theta)) \sin^{2n}(\theta) d\theta. \quad (\text{C3})$$

Appendix D: Taylor series truncation bounds

Let us introduce some notation that we use throughout this appendix. For a function $h: \mathbb{R} \rightarrow \mathbb{C}$ that is analytic in a neighborhood of 0 so that $h(y) = \sum_{k=0}^{\infty} b_k y^k$ we denote by $\|h\|_1 := \sum_{k=0}^{\infty} |b_k|$ the sum of the absolute values of the Taylor coefficients.

Now we prove our result on the truncation error based on Taylor series expansion, which we restate below:

Theorem 2. Let $b > 0$ and $f(x_0 + x) = \sum_{k=0}^{\infty} a_k x^k$ for every $x \in (-b, b)$ and suppose $\sum_{k=0}^{\infty} |a_k| b^k \leq B$. Then $g(y) := f(x_0 + \frac{2b}{\pi} \arcsin(y)) = \sum_{k=0}^{\infty} c_k y^k$ is such that $\sum_{k=0}^{\infty} |c_k| \leq B$, thus for $\nu \in (0, 1]$ and $T \geq \ln(B/\delta)/\nu$ we have for all $y \in [-1 + \nu, 1 - \nu]$:

$$\left| g(y) - \sum_{k=0}^{T-1} c_k y^k \right| \leq \delta.$$

Proof. The proof is inspired by [54, Lemma 37] where it is noted that $\| \frac{2}{\pi} \arcsin(y) \|_1 = 1$. This implies that

$$\begin{aligned} \|g(y)\|_1 &= \left\| f\left(x_0 + \frac{2b}{\pi} \arcsin(y)\right) \right\|_1 \\ &= \left\| \sum_{k=0}^{\infty} a_k \left(\frac{2b}{\pi} \arcsin(y)\right)^k \right\|_1 \\ &\leq \sum_{k=0}^{\infty} |a_k| \left\| \left(\frac{2b}{\pi} \arcsin(y)\right)^k \right\|_1 \\ &\leq \sum_{k=0}^{\infty} |a_k| \left\| \frac{2b}{\pi} \arcsin(y) \right\|_1^k \\ &= \sum_{k=0}^{\infty} |a_k| b^k \\ &\leq B, \end{aligned}$$

therefore we have for all $y \in [-1 + \nu, 1 - \nu]$:

$$\begin{aligned} \left| g(y) - \sum_{k=0}^{T-1} c_k y^k \right| &= \left| \sum_{k=T}^{\infty} c_k y^k \right| \\ &= |y|^T \left| \sum_{k=T}^{\infty} c_k y^{k-T} \right| \\ &\leq |y|^T \sum_{k=T}^{\infty} |c_k| \\ &\leq (1 - \nu)^T B \\ &\leq \exp(-\nu T) B \\ &\leq \delta. \end{aligned} \quad \square$$

Using this theorem we can give analytical bounds on the degree required for approximating the standard normal distribution as follows:

Corollary 1. Let $\beta, \delta > 0$, then there is a degree $d \leq \frac{\frac{\beta\pi^2}{8} + \ln(1/\delta)}{1 - \sin(1)} - 1$ polynomial $P(y)$ such that for every $y \in [-\sin(1), \sin(1)]$ we have that

$$\left| \exp\left(-\frac{\beta}{2} \arcsin^2(y)\right) - P(y) \right| \leq \delta. \quad (\text{D1})$$

Proof. We will apply Theorem 2 with setting $b = \frac{\pi}{2}$. For this observe that $\exp(-\frac{\beta}{2} x^2) = \sum_{k=0}^{\infty} \left(-\frac{\beta}{2}\right)^k \frac{x^{2k}}{k!}$ and

$\sum_{k=0}^{\infty} \left(\frac{\beta}{2}\right)^k \frac{\left(\frac{\pi}{2}\right)^{2k}}{k!} = \sum_{k=0}^{\infty} \frac{\left(\frac{\beta\pi^2}{8}\right)^k}{k!} = \exp\left(\frac{\beta\pi^2}{8}\right) =: B$. Consider the truncated Taylor series $P(y) = \sum_{k=0}^{T-1} c_k y^k$ of $\exp\left(-\frac{\beta}{2} \arcsin^2(y)\right)$ for $T \geq \frac{\frac{\beta\pi^2}{8} + \ln(1/\delta)}{1 - \sin(1)}$. By Theorem 2 we get that Equation (D1) holds. \square

Similarly, we get analytical bounds on the degree required for approximating the Kaiser window function $W_{\beta}(x) = \frac{I_0(\beta\sqrt{1-x^2})}{I_0(\beta)}$:

Corollary 2. Let $\beta, \delta > 0$, then there is a degree $d \leq \frac{\frac{\beta + \ln(1/\delta)}{1 - \sin(1)} - 1$ polynomial $P(y)$ such that for every $y \in [-\sin(1), \sin(1)]$ we have that

$$|W_{\beta}(\arcsin(y)) - P(y)| \leq \delta. \quad (\text{D2})$$

Proof. We will apply Theorem 2 with setting $b = \frac{\pi}{2}$. To compute an upper bound B we observe that the smallest possible value of B is given by $\|W_{\beta}(\frac{\pi}{2}x)\|_1$. To analyze this quantity let us recall Equation (C1) stating that $I_0(z) = G(z^2)$ for the entire function $G(z) = \sum_{k=0}^{\infty} \frac{(z/4)^k}{(k!)^2}$. This means that $W_{\beta}(x) = \frac{G(\beta^2(1-x^2))}{G(\beta^2)}$ so

$$\|W_{\beta}\left(\frac{\pi}{2}x\right)\|_1 = \left\| G\left(\beta^2\left(1 - \frac{\pi^2}{4}x^2\right)\right) \right\|_1 / G(\beta^2) \quad (\text{D3})$$

$$= \left\| \sum_{k=0}^{\infty} \frac{(\beta^2(1 - \frac{\pi^2}{4}x^2)/4)^k}{(k!)^2} \right\|_1 / G(\beta^2) \quad (\text{D4})$$

$$\leq \sum_{k=0}^{\infty} \frac{\| \beta^2(1 - \frac{\pi^2}{4}x^2)/4 \|_1^k}{(k!)^2} / G(\beta^2) \quad (\text{D5})$$

$$= \sum_{k=0}^{\infty} \frac{(\beta^2(1 + \frac{\pi^2}{4})/4)^k}{(k!)^2} / G(\beta^2) \quad (\text{D6})$$

$$\leq \sum_{k=0}^{\infty} \frac{((4\beta^2)/4)^k}{(k!)^2} / G(\beta^2) \quad (\text{D7})$$

$$= \frac{G(4\beta^2)}{G(\beta^2)} = \frac{I_0(2\beta)}{I_0(\beta)} \leq \exp(\beta), \quad (\text{D8})$$

where the last inequality follows from the integral representation of Bessel functions [53, Eq. (9.6.19)]:

$$\begin{aligned} I_0(2\beta) &= \frac{1}{\pi} \int_0^{\pi} \exp(2\beta \cos(\theta)) d\theta \\ &\leq \frac{1}{\pi} \int_0^{\pi} \exp(\beta \cos(\theta)) \exp(\beta) d\theta \\ &= I_0(\beta) \exp(\beta). \end{aligned}$$

Finally, consider the truncated Taylor series $P(y) = \sum_{k=0}^{T-1} c_k y^k$ of $W_{\beta}(\arcsin(y))$ for $T \geq \frac{\beta + \ln(1/\delta)}{1 - \sin(1)}$. By Theorem 2 we get that Equation (D2) holds. \square

Note that the above proofs are constructive in the sense that they also enable explicitly computing approximating polynomials by (approximately) computing the

coefficients of the Taylor series. Those coefficients can be computed for example utilizing the Taylor series of $\arcsin(x) = \sum_{\ell=0}^{\infty} \binom{2\ell}{\ell} \frac{2^{-2\ell}}{2\ell+1} x^{2\ell+1}$.

Appendix E: Analysis of filling fractions

Lemma 4. Consider the functions $\exp(-\frac{\beta}{2}x^2)$ and $W_{\beta}(x)$ on the interval $[-1, 1]$ for some $\beta \geq 0$, then $f(x) \geq 1 - \frac{\beta}{2}x^2$ and so the filling fraction satisfies

$$\mathcal{F}_f^{[\infty]} \geq \begin{cases} \frac{1}{\sqrt[3]{2}}, & \text{for } \beta \leq 2 \\ \frac{1}{\sqrt[4]{2\beta}}, & \text{for } \beta \geq 2. \end{cases} \quad (\text{E1})$$

Proof. Since $\exp(x)$ is a convex function we have $\exp(x) \geq 1 + x$ and thus $\exp(-\frac{\beta}{2}x^2) \geq 1 - \frac{\beta}{2}x^2$.

Now we prove that $W_{\beta}(x) \geq 1 - \beta x^2/2$ by observing that both functions are even, and they take value 1 at $x = 0$. Thus, for showing the inequality it suffices to show that $K'_{\beta}(x) \geq -\beta x$ for every $x \in (0, 1)$. We have that

$$K'_{\beta}(x) = -\beta x \frac{I_1(\beta\sqrt{1-x^2})}{\sqrt{1-x^2}I_0(\beta)},$$

so it suffices to show that $g(y) := \frac{I_1(\beta y)}{yI_0(\beta)} \leq 1$ for $y \in (0, 1)$. Now $g(1) = I_1(\beta)/I_0(\beta) \leq 1$ where the inequality follows from the integral representation of Bessel functions (C2). So it suffices to show that $g'(y) \geq 0$ for $y \in (0, 1)$. As $g'(y) = (\beta I_2(\beta y))/(yI_0(\beta))$, this holds since both $\beta/(yI_0(\beta)) \geq 0$ and $I_2(\beta y) \geq 0$ follows from (C3).

If $\beta \leq 2$ it follows that $\int_{-1}^1 f(x)^2 dx \geq \int_{-1}^1 (1 - \frac{\beta}{2}x^2)^2 dx = 2 - \frac{2}{3}\beta + \frac{\beta^2}{10} > 1$, and if $\beta \geq 2$ it follows that $\int_{-1}^1 f(x)^2 dx \geq \int_{-\sqrt{\frac{2}{\beta}}}^{\sqrt{\frac{2}{\beta}}} (1 - \frac{\beta}{2}x^2)^2 dx = \frac{16}{15}\sqrt{\frac{2}{\beta}} \geq \sqrt{\frac{2}{\beta}}$. \square

Lemma 5. Let $\beta \geq 0$ and let $f(x)$ be either $\exp(-\frac{\beta}{2}x^2)$ or $W_{\beta}(x)$. If $N \geq \sqrt{\beta}$ and $|\tilde{f}(\bar{x}) - f(\bar{x})| \leq \frac{1}{4}$ for all discrete evaluation points \bar{x} then we have $\mathcal{F}_{\tilde{f}}^{[N]} = \Omega(\frac{1}{\sqrt[4]{\beta+1}})$.

Proof. Consider the interval $I = [-\frac{1}{\sqrt{\beta}}, \frac{1}{\sqrt{\beta}}] \cap [-1, 1]$. For all $\bar{x} \in I$ we have $\tilde{f}(\bar{x}) \geq f(\bar{x}) - \frac{1}{4} \geq \frac{3}{4} - \frac{\beta}{2}\bar{x}^2 \geq \frac{1}{4}$, where

the first inequality comes from Lemma 4. Therefore,

$$\left(\mathcal{F}_{\tilde{f}}^{[N]}\right)^2 \geq \frac{\sum_{\bar{x} \in I} |\tilde{f}(\bar{x})|^2}{N|\tilde{f}|_{\max}^2} \geq \frac{\sum_{\bar{x} \in I} (\frac{1}{4})^2}{N(\frac{5}{4})^2} = \Omega\left(\frac{1}{\sqrt{\beta+1}}\right). \quad \square$$

Appendix F: Asymptotic analysis of Gaussian and Kaiser-window state preparation

Here we prove Theorem 3, which we restate below:

Theorem 3. Let $f_{\beta}(x)$ be either $\exp(-\frac{\beta}{2}x^2)$ or $W_{\beta}(x)$. If $\varepsilon \in (0, \frac{1}{2})$ and $2^n \geq \sqrt{\beta} \geq 0$, then we can prepare the corresponding Gaussian / Kaiser window state on n qubits up to ε -precision with gate complexity

$$\mathcal{O}\left(n\sqrt[4]{\beta+1}(\beta + \log(1/\varepsilon))\right). \quad (12)$$

For Gaussian states $f_{\beta}(x) = \exp(-\frac{\beta}{2}x^2)$ if $\beta \geq \log(1/\varepsilon)$ this complexity can be further improved to

$$\mathcal{O}\left(n \log^{\frac{5}{4}}(1/\varepsilon)\right). \quad (13)$$

Proof. This follows from Theorem 1. Because f is even, we use the modified block-encoding to begin with, namely $A := \sum_{x=-\frac{N}{2}}^{\frac{N}{2}-1} \sin(2x/N)|x\rangle\langle x|$. This does not affect the validity of our earlier analysis but enables us setting $x_0 = 0$ in Theorem 2. For applying this general result we first invoke our filling-fraction bounds Lemma 4 and Lemma 5 ensuring that $\text{Min}\left(\mathcal{F}_f^{[N]}, \mathcal{F}_{\tilde{f}}^{[N]}\right) = \Omega(\frac{1}{\sqrt[4]{\beta+1}})$. Then Corollary 1 and Corollary 2 implies that we can find a degree $\mathcal{O}(\beta + \log(1/\delta))$ approximating polynomial that has accuracy $\delta = \varepsilon \cdot \text{Min}\left(\mathcal{F}_f^{[N]}, \mathcal{F}_{\tilde{f}}^{[N]}\right) = \Omega(\frac{\varepsilon}{\sqrt[4]{\beta+1}})$, proving Equation (12).

Then Equation (13) follows from Equation (12) by observing that the function $\exp(-\frac{\beta}{2}x^2)$ is $0.5\varepsilon \cdot \text{Min}\left(\mathcal{F}_f^{[N]}, \mathcal{F}_{\tilde{f}}^{[N]}\right)$ -close to 0 for $x \gg \sqrt{\frac{2}{\beta} \ln\left(\frac{\sqrt[4]{\beta+1}}{\varepsilon}\right)} = \mathcal{O}\left(\sqrt{\frac{\log(1/\varepsilon)}{\beta}}\right)$ so we can assume without loss of generality that our approximation $\tilde{f}(x)$ is 0 for such large values. But then the task reduces to preparing a Gaussian state with $\beta' = \Theta(\log(1/\varepsilon))$ after rescaling $x \rightarrow x'$ so that $x \approx x' \cdot \sqrt{\frac{\log(1/\varepsilon)}{\beta}}$ and adjusting the value of N' appropriately. Note that by choosing the constants appropriately we can even ensure that N' remains a power of 2. \square